

# ENERGETIC EFFICIENCY OF MIXING AND MASS TRANSFER IN SINGLE PHASE AND TWO-PHASE SYSTEMS

Jerzy Bałdyga\*, Magdalena Jasińska

Warsaw University of Technology, Faculty of Chemical and Process Engineering, ul. Waryńskiego 1, Warsaw, Poland

*Dedicated to Prof. Leon Gradoń on the occasion of his 70th birthday*

In this work a concept of energetic efficiency of mixing is presented and discussed; a classical definition of mixing efficiency is modified to include effects of the Schmidt number and the Reynolds number. Generalization to turbulent flows is presented as well. It is shown how the energetic efficiency of mixing as well as efficiencies of drop breakage and mass transfer in two-phase liquid-liquid systems can be identified using mathematical models and test chemical reactions. New expressions for analyzing efficiency problem are applied to identify the energetic efficiency of mixing in a stirred tank, a rotor stator mixer and a microreactor. Published experimental data and new results obtained using new systems of test reactions are applied. It has been shown that the efficiency of mixing is small in popular types of reactors and mixers and thus there is some space for improvement.

**Keywords:** chemical test reactions, energetic efficiency, mass transfer, mixing

## 1. INTRODUCTION

In this work the authors are concerned with the influence of mixing on the course of complex chemical reactions in single phase liquid systems and two-phase liquid-liquid systems. This problem is considered in the chemical reaction engineering literature (Bałdyga and Bourne, 1999; Bourne, 2003; Levenspiel, 1972) from two related points of view. First of all the design and performance of chemical reactors should enable to run chemical reactions with the highest possible selectivity. On the other hand, complex chemical reactions can be used as test reactions, to investigate the efficiency of mixing. Using test reactions one can characterize the level of mixedness (intensity of segregation, time constants for mixing) and use this information to improve the performance of processes carried out in the reactor. The time constant for turbulent mixing can be defined as the time scale of decay of the concentration variance of the passive scalar,  $i$ .

$$\tau_M = \frac{\overline{(c_i - \bar{c}_i)^2}}{d(c_i - \bar{c}_i)^2} \quad (1)$$

For effective laminar mixing by fluid elongation, one can define the characteristic mixing time (Bałdyga and Bourne, 1986) by

$$\tau_M = \frac{1}{2\dot{\gamma}} \arcsin h(0.76\dot{\gamma}\delta_0^2/D_i) \quad (2)$$

\*Corresponding author, e-mail: J.Baldyga@ichip.pw.edu.pl

where  $\dot{\gamma}$  is the rate of elongation and  $\delta_0$  represents original thickness of the slab to be elongated. In the case of turbulent mixing the rate of elongation can be expressed as  $(\varepsilon/\nu)^{1/2}$  and the slab thickness expressed using the Kolmogorov microscale,  $\lambda_K$ . Then the mixing time can be expressed by the Corrsin (1964) equation

$$\tau_M \cong \frac{1}{2} \left( \frac{\nu}{\varepsilon} \right)^{1/2} \ln(Sc) \quad Sc \gg 1 \quad (3)$$

When both the inertial-convective and viscous-convective subranges of the concentration spectrum exist then the time constant for mixing reads (Corrsin, 1964):

$$\tau_M \cong \frac{2\Lambda_c^{2/3}}{\varepsilon^{1/3}} + \frac{1}{2} \left( \frac{\nu}{\varepsilon} \right)^{1/2} \ln(Sc) \quad Sc \gg 1 \quad (4)$$

where the relaxed integral scale for turbulent fluctuations of concentration,  $\Lambda_c$ , is proportional to the scale of the large, energy containing eddies,  $L$ ,  $\Lambda_c \cong L/2$ .

The process of mixing between elongated slabs in laminar flow or in the viscous-convective and viscous-diffusive subranges of turbulence can be represented by the rate of creation of the intermaterial area per unit volume,  $a_v$  [ $\text{m}^{-1}$ ], as given by (Ottino, 1980):

$$\left| \frac{1}{a_v} \frac{da_v}{dt} \right| = \text{eff}(t) (\bar{D} : \bar{D})^{1/2} \quad (5)$$

$$\bar{D} = \frac{1}{2} \left[ \text{grad}(\bar{u}) + \text{grad}(\bar{u})^T \right] \quad (6)$$

that is defined using the velocity gradient,  $\text{grad}(\bar{u})$ .

Equation (5) depicts the fact that orientation of the intermaterial area with respect to the principle axes of deformation determines the effectiveness of mixing. It characterises the ratio of energy really applied to increase the intermaterial area to the whole energy dissipated during the flow. Using this concept one can define the efficiency of mixing using either a definition proposed by (Ottino, 1980) for 2D systems,

$$\text{eff}(t) = \frac{1}{a_v} \frac{da_v}{dt} \left( \frac{\varepsilon_T}{2\nu} \right)^{-1/2} = -\frac{1}{\lambda} \frac{d\lambda}{dt} \quad (7)$$

or a similar definition published by Rozeń (2008) for 3D deformation

$$\text{eff}(t) = \frac{1}{a_v} \frac{da_v}{dt} \left( \frac{\varepsilon_T}{3\nu} \right)^{-1/2} = -\frac{1}{\lambda} \frac{d\lambda}{dt} \quad (8)$$

where  $\varepsilon_T$  [ $\text{m}^2\text{s}^{-3}$ ] represents the total rate of energy dissipation per unit mass and  $\lambda$  is the slab or striation thickness that is directly related to  $a_v$ , namely  $\lambda = a_v^{-1}$ . In this work the average values of efficiency during residence time  $t$  in the mixer will be considered.

## 2. THEORETICAL ASPECTS OF EFFICIENCY OF MICROMIXING

Equations (5) to (8) describe just fluid deformation but they do not consider mixing on the molecular scale. This means that intensity of segregation (a normalized variance of the passive scalar tracer) stays equal to unity during mixing. To illustrate an influence of the local flow structure on mixing, consider a spot of contaminant of finite molecular diffusivity,  $D_i$ , which is transported, deformed and rotated.

Following Tennekes and Lumley (1972) and Bałdyga and Bourne (1999), one can start from the conservation equation for the concentration,  $c$

$$\frac{\partial c}{\partial t} + u_j \frac{\partial c}{\partial x_j} = D_i \frac{\partial^2 c}{\partial x_j^2} \quad (9)$$

and assume that the spot size is smaller than the Kolmogorov microscale  $\lambda_K$ . The spot position is determined by the position of the Lagrangian point  $\vec{X}$  that can be interpreted as the centre of mass of the spot. One can write the differential mass balance in a local coordinate system  $(\xi_1, \xi_2$  and  $\xi_3)$  attached to the Lagrangian point  $\vec{X}$ , where  $\vec{\xi} = \vec{x} - \vec{X}$  is the position vector in the moving frame. The fluid element is assumed to be smaller than the Kolmogorov microscale, hence the relative motion  $\vec{u}(\vec{\xi}) = \vec{u}(\vec{x}) - \vec{u}(\vec{X}) - \vec{\omega} \times \vec{\xi}$  is described by a linear relation, leading to

$$\frac{\partial c}{\partial t} + \xi_j \frac{\partial u_i}{\partial \xi_j} \frac{\partial c}{\partial \xi_i} = D \frac{\partial^2 c}{\partial \xi_i^2} \quad (10)$$

Treating now the concentration of the tracer substance as a three-dimensional probability density function one can characterize the shape of our spot by using the concentration moments (Tennekes and Lumley, 1972).

$$I_{kl} = \frac{\int \int \int \xi_k \xi_l c(\vec{\xi}, t) d\xi_1 d\xi_2 d\xi_3}{\int \int \int c(\vec{\xi}, t) d\xi_1 d\xi_2 d\xi_3} \quad (11)$$

This definition allows the diagonal moment  $I_{kk}$ , to be used as a quantity proportional to the square of the penetration distance of the contaminant in the “ $k$ ” direction. The shape of the spot can be characterized by comparing the diagonal moments  $I_{11}$ ,  $I_{22}$  and  $I_{33}$

$$\delta_1^2 : \delta_2^2 : \delta_3^2 = I_{11} : I_{22} : I_{33} \quad (12)$$

whereas the sum of diagonal components  $I = I_{kk} = I_{11} + I_{22} + I_{33}$  is proportional to the square of the average spot radius. From Eqs. (10) and (11) one gets after transformation

$$\frac{dI_{kk}}{dt} - 2(s_{km} + \Omega_{km})I_{km} = 2D\delta_{kk} \quad (13)$$

where  $s_{km}$  and  $\Omega_{km}$  represent the pure deformation and rotation tensors, respectively.

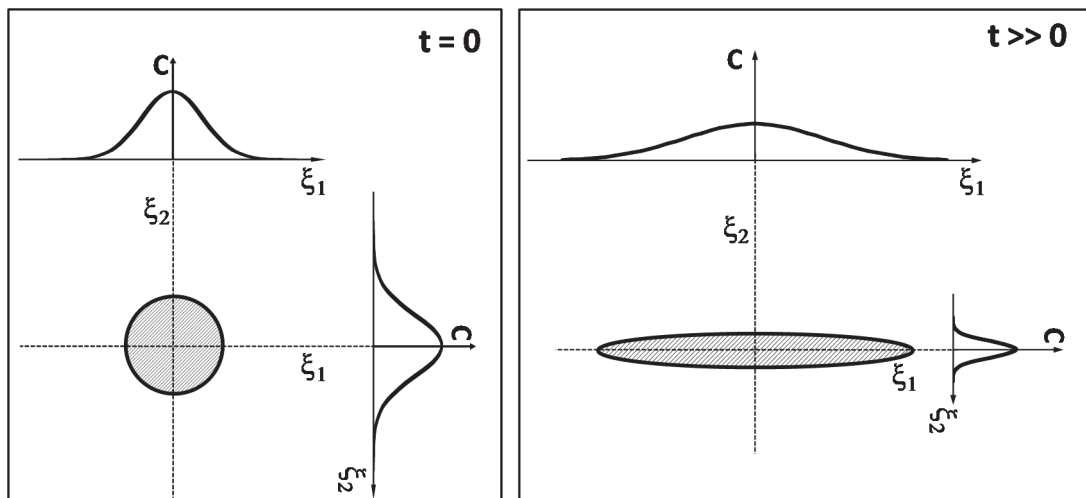


Fig. 1. Effect of stretching on spreading of the contaminant due to molecular diffusion

Equation (13) shows effects of deformation and rotation on spreading of the contaminant. To show relation between fluid deformation and mixing on molecular scale one can neglect effects of rotation, and follow spreading of the contaminant in the 2-dimensional flow, as shown in Fig. 1.

Equation (13) reduces then to

$$\frac{dI_{11}}{dt} - 2sI_{11} = 2D_i \quad (14)$$

$$\frac{dI_{11}}{dt} + 2sI_{11} = 2D_i \quad (15)$$

which can be solved with initial conditions  $I_{11}(0) = \delta_0^2$  and  $I_{22}(0) = \delta_0^2$ , and  $s = \text{const.}(\varepsilon/\nu)^{1/2}$ , yielding

$$I_{SD} = I_{11} + I_{22} = 2\delta_0^2 \cosh(2st) + 2\frac{D_i}{s} \sinh(2st) \quad (16)$$

Notice that definitions (7) and (8) consider only the first term on the RHS of Eq.(16). When there is no deformation ( $s = 0$ ), Eq.(16) reduces to

$$I_D = I_{11} + I_{22} = 2\delta_0^2 + 4D_i t \quad (17)$$

To present effect of deformation on mixing one can plot the ratio  $I_{SD}/I_D$  versus dimensionless time,  $s \cdot t$  for  $\delta_0 = 0$ , as shown in Fig. 2.

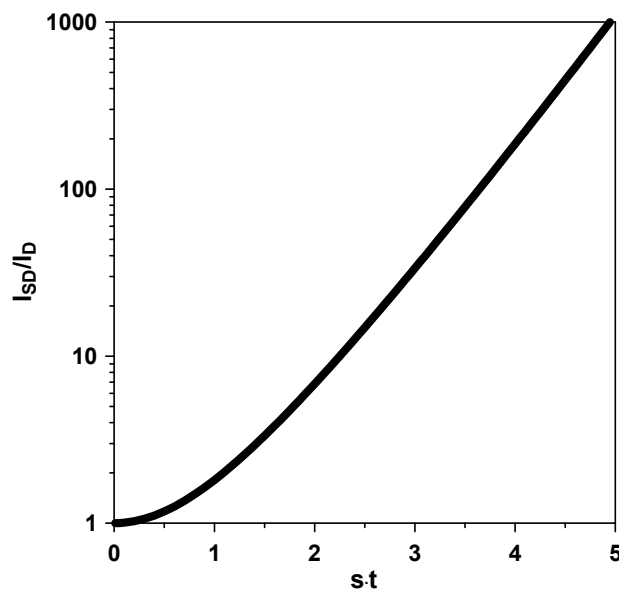


Fig. 2. Effect of fluid deformation on spreading of the contaminant

Figure 2 shows a dominating effect of stretching on spreading due to molecular diffusion. If, however, rotation effects are not neglected, and conditions presented in Fig. 1 are replaced by those given in Fig. 3, then the resulting solution will look different, as shown in Fig. 4. Figure 4 clearly shows that the growth of the spot of a contaminant is retarded by rotation; when rotation is small, the growth is still exponential, but with the resulting rate of stretching, e.g.  $\dot{\gamma}'_1$ , smaller than  $s_{11} = s$ . For intensive rotation the spot is turned to a new orientation before the gradients have opportunity to increase and accelerate molecular diffusion.

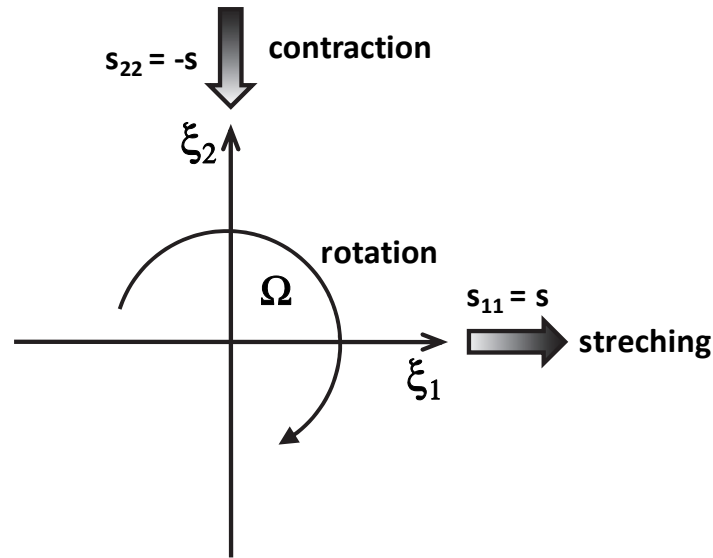


Fig. 3. The flow field including rotation

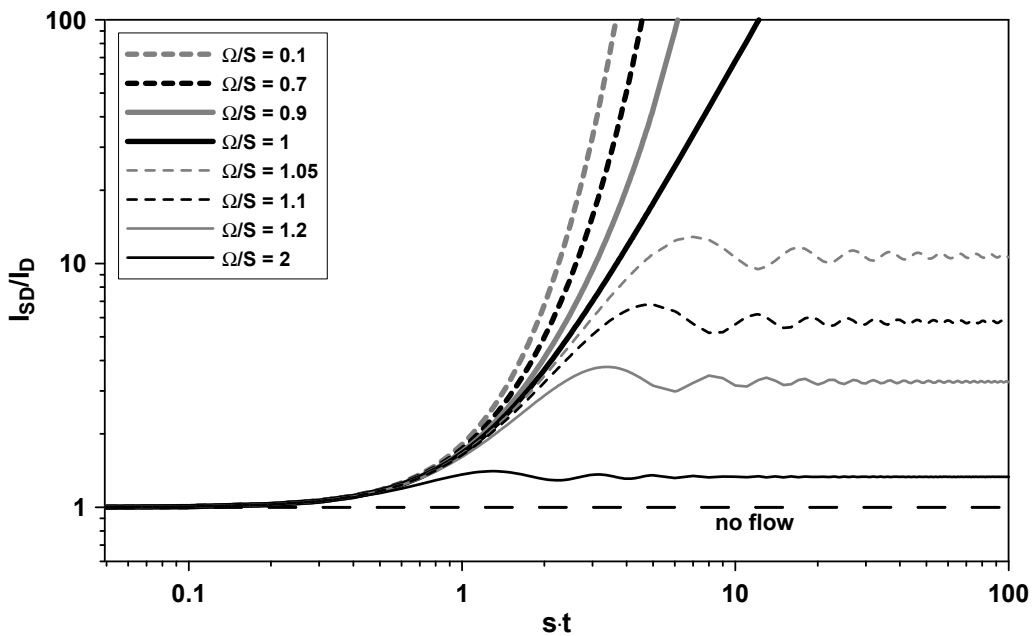


Fig. 4. Effects of stretching and rotation on spreading of the contaminant

Equation (13) for  $\Omega/s < 1$  can be presented in the local frame of reference  $(\xi'_1, \xi'_2)$  such that the off-diagonal moments vanish, and Eq. (13) is replaced by

$$\frac{1}{I'_{ii}} \frac{dI'_{ii}}{dt} = 2 \left[ \frac{D}{I'_{ii}} + \dot{\gamma}'_i(\vec{x}, t) \right] \quad (18)$$

where  $\dot{\gamma}'_1 = \beta \cdot s = \beta \cdot \left(\frac{\varepsilon}{2\nu}\right)^{1/2}$  and  $\dot{\gamma}'_2 = -\beta \cdot s = \beta \cdot \left(\frac{\varepsilon}{2\nu}\right)^{1/2}$  with  $0 \leq \beta \leq 0$ . The coefficient  $\beta$  is equivalent to the efficiency  $eff$  defined by Eq. (7).

As mentioned earlier, Eqs. (5) to (8) are based on analysis of fluid deformation but they do not consider mixing on the molecular scale. In what follows let us consider turbulent mixing and include effects of molecular diffusion. This should lead to a more realistic definition of energetic efficiency. Considering that the slab or striation thickness is directly related to  $a_v$ , namely  $\lambda = a_v^{-1}$ , we get from Eqs. (5) and (8)

$$\frac{1}{\lambda} \frac{d\lambda}{dt} = -eff(t) \cdot \left(\frac{\varepsilon}{3\nu}\right)^{1/2} \quad (19)$$

When Eq. (19) is integrated from the Kolmogorov microscale  $\lambda_K = \frac{\nu^{3/4}}{\varepsilon^{1/4}} = k_K^{-1}$  to the Batchelor microscale,  $\lambda_B = \frac{\nu^{1/4} D^{1/2}}{\varepsilon^{1/4}} = k_B^{-1}$  the latter representing a cut-off of the spectrum due to molecular diffusion as shown in Fig. 5, then the time of decreasing  $\lambda$  from  $\lambda_K$  to  $\lambda_B$  corresponds to the mixing time,  $\tau_M$ . This results in the new equation for efficiency of micromixing:

$$eff = \frac{\sqrt{3}}{2} \frac{\left(\frac{\nu}{\varepsilon}\right)^{1/2} \ln(Sc)}{\tau_M} \quad (20)$$

Once the characteristic time scale for mixing is measured one can calculate the efficiency of mixing from Eq.(20). In this section we identify efficiency of mixing based on available in the mixing literature models of mixing on the molecular scale.

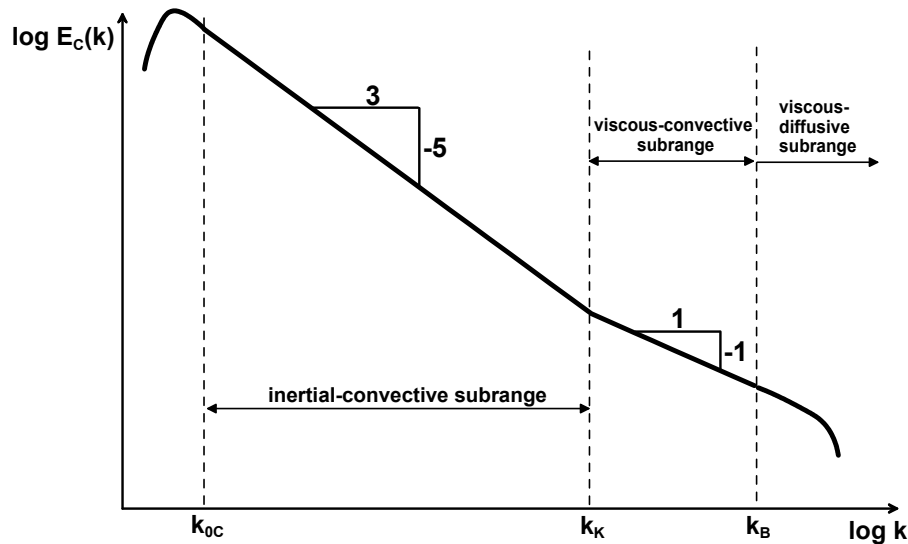


Fig. 5. Spectrum of concentration variance in liquids with very large Schmidt number at very high Reynolds number

Let us start from mixing in the viscous-convective and viscous-diffusive subranges of turbulence, Eq. (3). In Eq. (3) it was assumed that the rate of strain is equal to  $(\varepsilon/\nu)^{1/2}$ . We can replace now the prefactor for the rate of strain more precisely: based on Taylor's equation one gets  $|du/dx| = (2\varepsilon/15\pi\nu)^{1/2}$ , which leads to  $\tau_M \cong 2.42(\nu/\varepsilon)^{1/2} \ln(Sc)$  instead of Eq. (3). A more exact expression including the effect of skewness factor was given by Batchelor (1980) for the characteristic rate of strain  $|du/dx| = 7S/(6\sqrt{15}) \cdot (\varepsilon/\nu)^{1/2}$  where  $S$  is the skewness factor. After substituting for  $S$  the value 0.6 we get  $|du/dx| = 0.151(\varepsilon/\nu)^{1/2}$  and

$$\tau_M \cong 3.3 \left(\frac{\nu}{\varepsilon}\right)^{1/2} \ln(Sc) \quad Sc \gg 1 \quad (21)$$

which after substitution to Eq. (20) results in  $eff = 0.26$ . A slightly less exact estimate for isotropic turbulence based on Taylor's equation results in  $eff = 0.36$ .

The results show that due to reorientation of the rate of strain tensor at a small scale in turbulent flow the efficiency of mixing  $eff = 1$  is not possible.  $eff = 1$  would be possible for continuous elongation of threads of fluid in 3D space without reorientation, which does not take place in turbulent flows.

Introducing now Batchelor's correction to Eq. (4) we get

$$\tau_M \cong \frac{2\Lambda_c^{2/3}}{\varepsilon^{1/3}} + 3.3\left(\frac{\nu}{\varepsilon}\right)^{1/2} \ln(\text{Sc}) \quad \text{Sc} \gg 1 \quad (22)$$

and substituting for the integral scale of concentration fluctuations the relaxed value,  $\Lambda_c \cong L/2$ ,

$$eff = \frac{\frac{\sqrt{3}}{2}\left(\frac{\nu}{\varepsilon}\right)^{1/2} \ln(\text{Sc})}{\frac{\Lambda_c^{2/3}}{\varepsilon^{1/3}} + 3.3\left(\frac{\nu}{\varepsilon}\right)^{1/2} \ln(\text{Sc})} = \frac{\frac{\sqrt{3}}{2}\left(\frac{\nu}{\varepsilon}\right)^{1/2} \ln(\text{Sc})}{1.26\frac{L^{2/3}}{\varepsilon^{1/3}} + 3.3\left(\frac{\nu}{\varepsilon}\right)^{1/2} \ln(\text{Sc})} = \frac{0.69 \ln(\text{Sc})}{\text{Re}_L^{1/2} + 2.6 \ln(\text{Sc})} \quad (23)$$

where  $\text{Re}_L = u'L/\nu$  is the Reynolds number based on the root-mean-square velocity fluctuation  $u'$  and the scale of the large, energy containing eddies,  $L$ . Equation (23) is based on the definition of efficiency given by Eq. (20). A special definition for turbulent mixing can be proposed when instead of  $\left(\frac{\varepsilon}{3\nu}\right)^{1/2}$  valid for laminar flow we will use after Batchelor (1980) the maximum possible rate of deformation for turbulent flow  $|du/dx| = 7S/(6\sqrt{15}) \cdot (\varepsilon/\nu)^{1/2}$ . Then efficiency for turbulent mixing,  $eff_2$ , defined as

$$eff_2 = \frac{3.3\left(\frac{\nu}{\varepsilon}\right)^{1/2} \ln(\text{Sc})}{\frac{\Lambda_c^{2/3}}{\varepsilon^{1/3}} + 3.3\left(\frac{\nu}{\varepsilon}\right)^{1/2} \ln(\text{Sc})} = \frac{3.3\left(\frac{\nu}{\varepsilon}\right)^{1/2} \ln(\text{Sc})}{1.26\frac{L^{2/3}}{\varepsilon^{1/3}} + 3.3\left(\frac{\nu}{\varepsilon}\right)^{1/2} \ln(\text{Sc})} = \frac{2.6 \ln(\text{Sc})}{\text{Re}_L^{1/2} + 2.6 \ln(\text{Sc})} \quad (24)$$

will take values between 0 and 1.

Figure 6 shows effects of the Reynolds number and the Schmidt number on mixing efficiency.

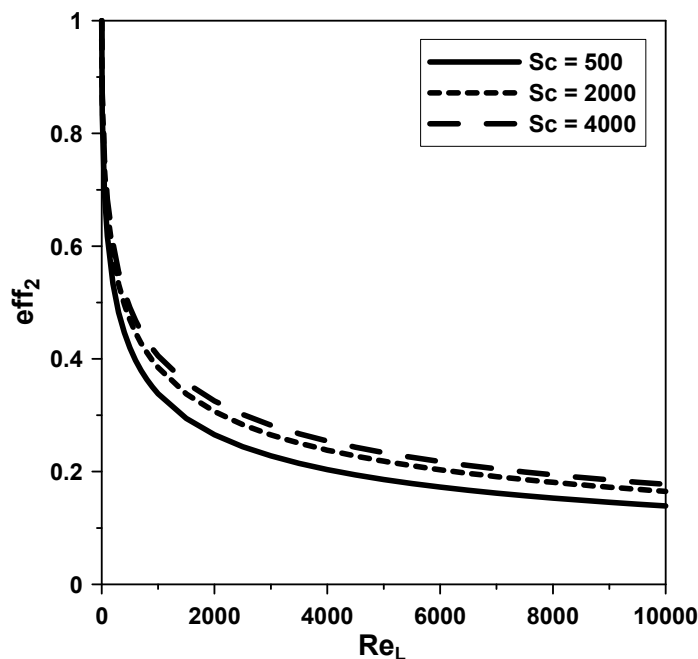


Fig. 6. Effects of the Reynolds and Schmidt numbers on efficiency of mixing

The efficiency of mixing decreases significantly with increasing the Reynolds number due to the increasing role of the inertial-convective mixing and increases slightly with increasing the Schmidt number. To run the process at high efficiency it is important to decrease the integral scale,  $\Lambda_c$ , in Eq. (22). When reagents are fed to the tank very slowly through the feeding nozzle of small diameter then one has  $\Lambda_c \ll L$  and its effect in Eq. (22) is negligible (see Bałdyga and Bourne (1999)). In such a case multiple feeding pipes are recommended to have a faster overall feeding rate.

For description of micromixing under such asymptotic conditions the Engulfment model is recommended. The model describes viscous-convective processes of building lamellar structures by engulfment and deformation.

When micromixing is controlled by a viscous-convective engulfment process, then the  $c_i$  concentration history can be calculated from the engulfment equations:

$$\frac{dc_i}{dt} = E(\langle c_i \rangle - c_i) + r_i \quad (25)$$

$$\frac{d(\delta V_i)}{dt} = E \cdot \delta V_i \quad (26)$$

with engulfment parameter  $E = 0.058 \left( \frac{\varepsilon}{\nu} \right)^{1/2}$ , that depends on flow conditions and fluid viscosity.  $\langle c_i \rangle$

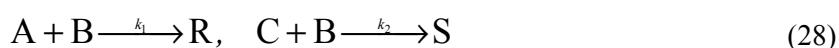
represents here the concentration of reactant  $i$  in the environment. For this model the efficiency as defined by Eq. (8) is equal to  $eff = 0.1$ . Because the E-model is easy to use and validated experimentally, we will treat the value predicted by this model as the reference one and define relative efficiency based on it. Of course it is always possible to express the absolute efficiency defined by Eqs. (7) or (8) by multiplying the efficiency identified using E-model by 0.1. In such a case the E-model, or any other model of this type, takes the role of an agent of efficiency identification. Notice that a somewhat similar approach was applied by Falk and Commenge (2010), where as a reference model the model for laminar mixing (Bałdyga and Bourne, 1986) was used in combination with the IEM model (Villermaux, 1986).

### 3. EXPERIMENTAL IDENTIFICATION OF MICROMIXING EFFICIENCY

The procedure to characterize efficiency of mixing includes modelling of effects of mixing on the course of the test chemical reactions using the E-model of micromixing (Bałdyga and Bourne, 1999). In the E-model the engulfment parameter,  $E = 0.058(\varepsilon/\nu)^{1/2}$  depends on the rate of energy dissipation,  $\varepsilon$ . One can construct then the calibration curve representing the theoretical dependence of the product distribution on the rate of energy dissipation. Having measured the value of product distribution one identifies then the rate of energy dissipation,  $\varepsilon$  as the theoretical reference value. Comparing the theoretical rate of energy dissipation,  $\varepsilon$  necessary to obtain the same product distribution,  $X_S$ , as the one observed in experiment under consideration, characterized by the rate of energy dissipation equal to  $\varepsilon_T$ , one can express the average efficiency of mixing,  $\overline{eff}$ , by

$$\overline{eff} = \left( \frac{\varepsilon}{\varepsilon_T} \right)^{1/2} \quad (27)$$

Let us consider the set of competing or parallel reactions as given by Eq. (28):



A good example of such a reacting system is competitive neutralization of hydrochloric acid and alkaline hydrolysis of monochloroacetate methyl or ethyl esters of monochloroacetic acid (Bałdyga and Bourne, 1999). In what follows in this section we use as a reference system the one given by Eq. (28) with  $A = \text{HCl}$ ,  $B = \text{NaOH}$ ,  $C = \text{CH}_2\text{ClCOOC}_2\text{H}_5$ ,  $R = \text{H}_2\text{O}$  or  $\text{NaCl}$ ,  $S = \text{C}_2\text{H}_5\text{OH}$  or  $\text{CH}_2\text{ClCOONa}$  and a new one, with  $C$  replaced by  $\text{CHCl}_2\text{COOC}_2\text{H}_5$  and thus  $S$  represented this time by  $\text{CHCl}_2\text{COONa}$ . To illustrate application of the test reactions, both experiments and simulations have been performed. Experiments were carried out using a semibatch stirred tank reactor of diameter  $T = 145$  mm, equipped with the Rushton type impeller of diameter  $D_{\text{imp}} = 50$  mm and 4 baffles of a width equal to 15 mm.

The product distribution was represented by the ratio of number of reacted moles of the ester to the number of moles of the base (B) for  $N_A = N_B = N_C$ .

$$X_S = \frac{\Delta N_C}{N_A} \quad (29)$$

The feeding of B solution to premixture A and C was so slow that there was no effect of feeding rate observed on the product distribution. In this situation the inertial-convective mixing is not active and one can expect  $\overline{eff} = \left(\frac{\varepsilon}{\varepsilon_T}\right)^{1/2} \cong 1$

Figure 7 shows that results of simulation with the E-model agree very well with experimental data, hence  $\varepsilon = \varepsilon_T$ . Notice that the relative efficiency based on comparison with the E-model is equal to 1, but the efficiency characterising E-model itself is 10%.

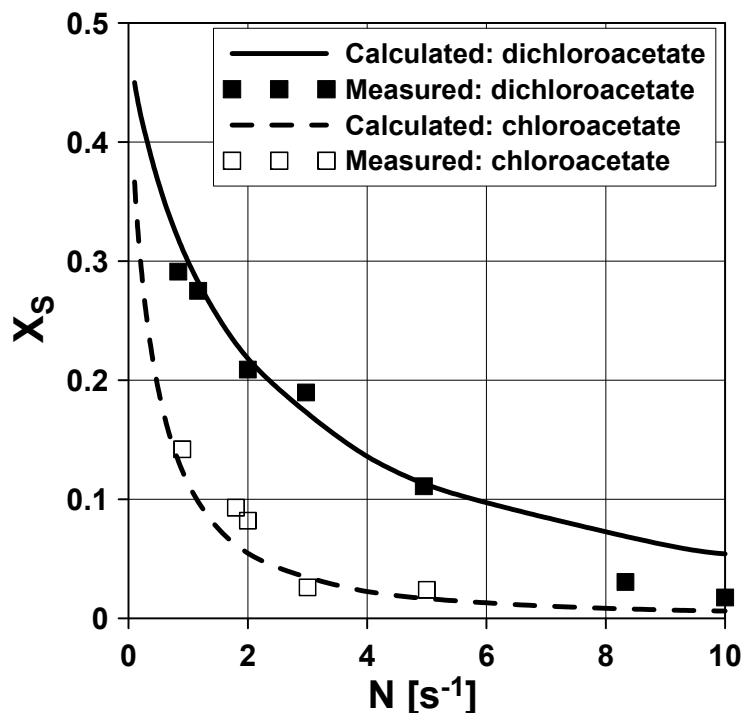
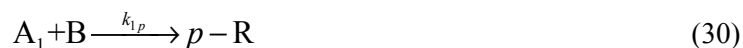


Fig. 7. Effect of agitation rate on selectivity  $X_S$  for ethyl chloroacetate and ethyl dichloroacetate;  $c_B = 1\text{M}$ ,  $c_{A0} = c_{C0} = 0.02\text{M}$ ,  $\alpha = 50$ , feeding position A close to the impeller

When as a system of the test reactions a simultaneous diazo-coupling between 1- and 2-naphtols and diazotized sulphanilic acid is applied (Bourne et al., 1992), two measures of product distribution can be used, one concentrating on the yield of secondary product  $S$  (a bisazo dye) and the other on the yield of the competitive product  $Q$  (a single monoazo dye).  $X_Q$  means then a fraction of the diazotized

sulphanilic acid converted into  $Q$  and similarly  $X_S$  presents a fraction of the diazotized sulphanilic acid converted into  $S$ .



$$X_S = 2c_S / (c_{oR} + c_{pR} + c_Q + 2c_S) \quad (35)$$

$$X_Q = c_Q / (c_{oR} + c_{pR} + c_Q + 2c_S) \quad (36)$$

where  $A_1$  denotes 1-naphthol,  $A_2$  is 2-naphthol,  $B$  represents diazotized sulphanilic acid,  $o-R$  and  $p-R$  are two mono-substituted dyes (ortho and para),  $S$  represents a bisazo dye and  $Q$  is a single monoazo dye.

Effects of energy dissipation  $\varepsilon$  and the volume ratio of reactants  $\alpha$  on  $X_S$  and  $X_Q$  as predicted by the E-model are presented in Fig. 8. To this end Eqs. (25) and (26) are applied together with the kinetics describing rates of reactions represented by Eqs. (30) to (36) (Baldyga and Bourne, 1999; Bourne et al., 1992). Notice that Fig. 8 has been constructed in a similar way as Fig. 7, just for different kinetics and without replacing the rate of energy dissipation by equivalent frequency of impeller. One can see that for high values of the rate of energy dissipation one should apply rather  $X_Q$  than  $X_S$  to interpret effects of mixing due to higher sensitivity to the rate of energy dissipation.

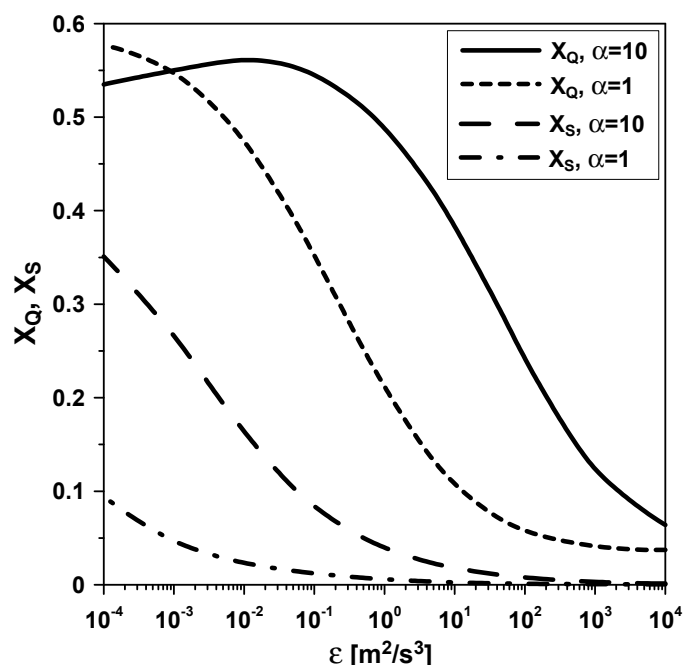


Fig. 8. Predicted effect of the energy dissipation rate,  $\varepsilon$ , on product distributions  $X_Q$  and  $X_S$ :

for  $\alpha = Q_A/Q_B = 1$ ,  $c_{A1,0} = 1.2 \text{ mol/m}^3$ ,  $c_{A2,0} = 2.4 \text{ mol/m}^3$ ,  $c_{B0} = 1 \text{ mol/m}^3$ ,  
 for  $\alpha = Q_A/Q_B = 10$ ,  $c_{A1,0} = 1.2 \text{ mol/m}^3$ ,  $c_{A2,0} = 2.4 \text{ mol/m}^3$ ,  $c_{B0} = 10 \text{ mol/m}^3$

As shown in Fig. 9, Fig. 8 can be used in what follows as a calibration curve, which based on experimentally determined  $X_Q$  values gives the smallest, “theoretical” values of the rate of energy

dissipation necessary to obtain experimental  $X_Q$ , that can be later compared with the energy really used in the experiment.

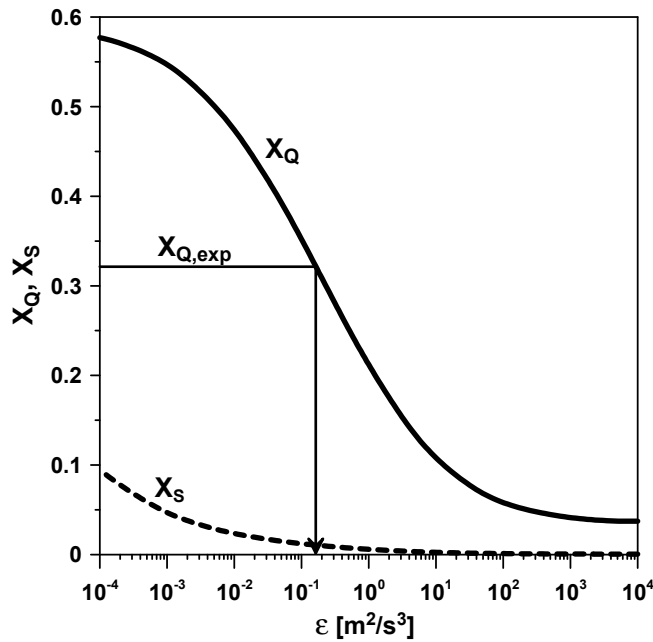


Fig. 9. Application of calibration curve

Applying this procedure to experimental data presented by (Jasińska et al., 2013a) for homogeneous mixing in a Silverson 150/250 MS rotor-stator mixer one obtains results shown in Fig. 10. The efficiency is calculated from Eq. (27) with the energy dissipation  $\varepsilon_T$  resulting from both, agitation and flow  $\varepsilon_T = \varepsilon_{N,Q}$ . In this paper the rate of energy dissipation  $\varepsilon_{N,Q}$  is calculated from the power number correlation (Jasińska et al., 2013a) and the rotor swept volume  $V_H$ .

$$N_P = 6.0 \cdot N_Q + 0.24 \quad (37)$$

where

$$N_Q = Q / (ND^3) \quad (38)$$

represents dimensionless flow rate.

The average rate of energy dissipation is thus given by Eq. (39)

$$\varepsilon_{N,Q} = N_P N^3 D^5 / V_H \quad (39)$$

One can see in Fig. 10 that as expected with increasing rotor speed the product distribution  $X_Q$  decreases, so mixing becomes faster. However, it becomes less efficient with increasing Re as well, in agreement with the theory, Eq. (24) and Fig. 6.

The same procedure has been applied to other systems, including microreactors (Malecha et al., 2009). It is interesting to compare results obtained for the rotor-stator device presented in Fig. 10 with similar results obtained in the serpentine microreactor are shown in Fig. 11.

The theoretical rate of energy dissipation was identified using the procedure presented in Figure 9 and the overall rate of energy dissipation was recalculated from measured pressure drop and flow rate,  $\varepsilon_{\Delta P} = Q\Delta P / (\rho V_R)$ . One can see from Figure 11 that in this case efficiency of mixing increases with increasing the Reynolds number. This happens because of destabilization of the laminar flow; at small Re number molecular diffusion controls mixing and energy is just used to move the fluid parallel to reactor walls. In a simple linear stable laminar shear flow the shearing motion will stretch and rotate

fluid elements, with consequences explained earlier. At higher Re numbers the flow is destabilised and faster mixing is induced by flow instability. Lamellar structures are first formed by unstable flow, then fluid deformation accelerates molecular diffusion and this effect increases with increasing Re. Figures 10 and 11 show that measured effects of the Reynolds number on mixing efficiency can help to identify mechanism of mixing.

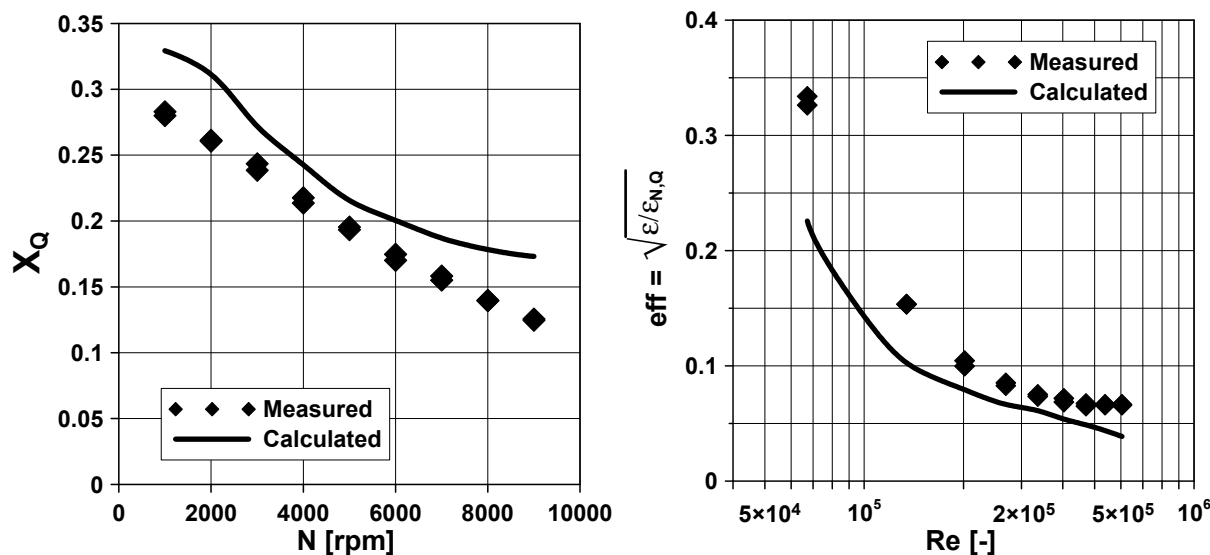


Fig. 10. Dependences of the product distribution  $X_Q$  on the rotor speed and efficiency of mixing  $eff$  on the Reynolds number,  $Re$

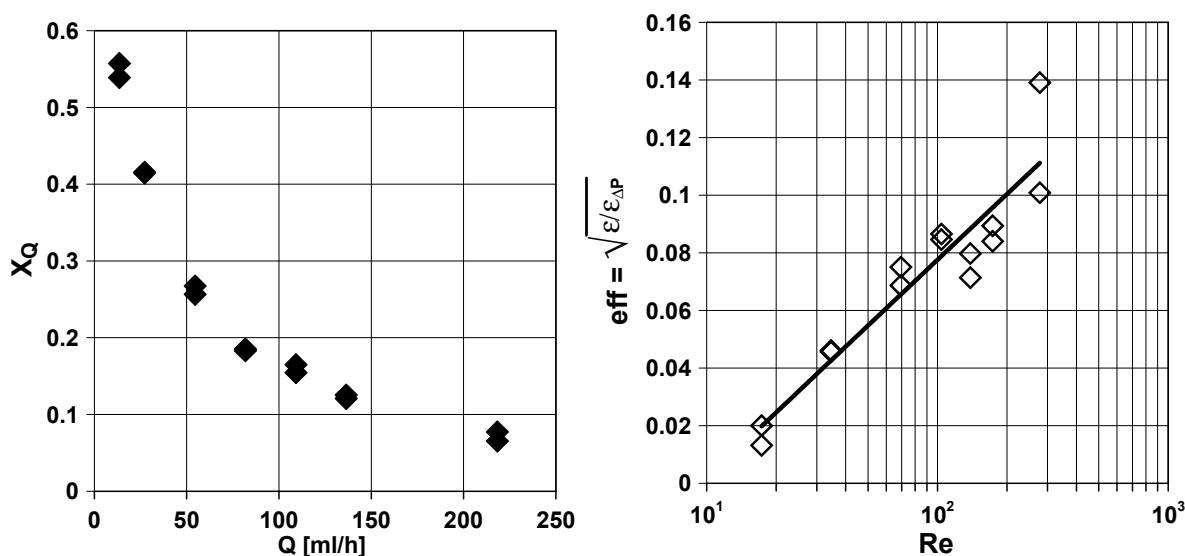


Fig. 11. Dependences of the measured product distribution  $X_Q$  on the flow rate and efficiency of mixing  $eff$  on the Reynolds number,  $Re$  (based on Malecha et al., 2009)

#### 4. MASS TRANSFER EFFICIENCY IN LIQUID-LIQUID SYSTEMS

Equations (20), (23) and (24) can be interpreted as the ratio of two time constants with the minimum possible time constant in the numerator and the real one in the denominator. Theoretical interpretation of efficiency of the mass transfer in liquid-liquid systems can be constructed in a similar way. The time constant for mass transfer can be defined as

$$\tau_D = \frac{1}{K_L a} \quad (40)$$

where  $K_L a$  represents the volumetric mass transfer coefficient, and

$$K_L = \left( \frac{1}{k_{Ld} \cdot P} + \frac{1}{k_{Lc}} \right)^{-1} \quad (41)$$

with  $k_{Ld}$  and  $k_{Lc}$  being mass transfer coefficients in the dispersed and continuous phase respectively and  $P$  is the equilibrium distribution coefficient between phases.

Then the energetic efficiency can be defined by

$$eff = \frac{\tau_{D,min}}{\tau_D} \quad (42)$$

For low solubility of the solute in the continuous phase one has  $P \gg 1$  and then  $K_L \cong k_{Lc}$ . This happens when an organic solute is dissolved in the organic dispersed phase and the aqueous solution represents the continuous phase as considered by Jasińska et al., (2013b).

Two aspects of the efficiency can be considered based on definition, Eq. (42): the first one is related to efficiency of drop breakage, the second one to efficiency of mass transfer.

Similarly as the E-model was chosen as a reference model for mixing in homogeneous systems, one can choose a reliable reference model for mass transfer. In this paper the value of  $k_{Lc} a$  will be calculated using the model of Favelukis and Levrenteva (2013),  $k_{Lc} = k_{FL}$ , which includes effects of drop deformation to the shape of prolate ellipsoid

$$k_{FL} a_{drop} = 4\pi R_{eq} D_i \sqrt{\frac{3}{2\pi(1+K)}} \left[ 1 - \frac{4(4+31K)Y}{315(1+K)} N_{Ca} \right] Pe^{1/2} \quad (43)$$

where  $Y = (19K+16)/(16K+16)$ . The capillary number and the Péclet number are defined using the equivalent radius, i.e. the radius of a sphere of equal volume to that of the deformed drop  $R = R_{eq} = d_{eq}/2$ . Using  $k_{FL} a_{drop}$  and the population balance to calculate the interfacial area per unit volume  $a$ ,  $a = 6\phi a_{drop} / (\pi d_{eq}^3)$ , one can determine  $k_{Lc} a = k_{FL} a$  and related time constant  $\tau_D$ .

Efficiency of drop breakage can be expressed by effect of drop size on the time constants for mass transfer,  $\tau_D$ . The time constant  $\tau_{D,min}$  in Eq. (42) can be interpreted as the shortest mass transfer time calculated from the model of Favelukis and Levrenteva (2003) using the maximum stable drop size  $d_d$ ,  $R_{eq} = d_d/2$ . The maximum stable drop size  $d_d$  can be estimated including intermittency effects using an equation given by Bałdyga and Podgórska (1998).

$$d_d = C_x^{1.54} L \left( \frac{\sigma}{\rho_c \varepsilon^{2/3} L^{5/3}} \right)^{0.93} \quad (44)$$

where  $L$  is the integral scale of turbulence,  $C_x = 0.23$ , and the rate of energy dissipation  $\varepsilon$  applied in Equations (43) and (44) represent the values really used in experiments. This gives

$$\tau_{D,min} = \frac{\pi d_d^3}{6\phi (k_{FL} a_{drop})_{R_{eq}=d_d/2}} \quad (45)$$

where  $\phi$  represents the mean value of the volume fraction of the organic, dispersed phase. Similar calculations but performed for  $R_{eq} = d_{32}/2$  give the time constant  $\tau_D$ .

$$\tau_D = \frac{\pi d_{32}^3}{6\phi(k_{FL}a_{drop})_{R_{eq}=d_{32}/2}} \quad (46)$$

Then efficiency of development of the interfacial area reads

$$eff_a = \left(\frac{d_d}{d_{32}}\right)^3 \cdot \frac{(k_{FL}a_{drop})_{R_{eq}=d_{32}/2}}{(k_{FL}a_{drop})_{R_{eq}=d_d/2}} = \frac{\tau_{D,\min}}{\tau_D} \quad (47)$$

The efficiency as given by Eq.(47) has been defined using the reference model represented by Eq. (44), similarly as the E-model has been used to determine efficiency of micromixing. As mentioned before, the E-model has been used as an agent necessary to identify the absolute efficiency as defined by Eqs. (7) and (8). One can define such absolute efficiency also in the case of development of the interfacial area,  $a$ .

The work  $dw$  done to expand the interfacial area  $dA$  can be presented as  $dw = \sigma dA$ . This leads directly to

$$\frac{da}{dt} = \frac{\rho\varepsilon'}{\sigma} \quad (48)$$

where  $\varepsilon'$  represents this part of mechanical energy that is used to increase an interfacial area.

For a continuous flow system with the mean residence time  $\bar{t}$  one has then

$$\Delta a = \frac{\rho\varepsilon'\bar{t}}{\sigma} \quad (49)$$

where  $\Delta a$  is an increase of the interfacial area between an inlet and an outlet of the system. Based on measured  $\Delta a$  one can calculate  $\varepsilon'$  and express efficiency of development of interfacial area as

$$eff'_a = \frac{\varepsilon'}{\bar{\varepsilon}} \quad (50)$$

where  $\bar{\varepsilon}$  is the average rate of energy dissipation in the system. However, the values of efficiency resulting from Eq.(50) are extremely low, which means that the application of Eq. (50) can be cumbersome.

Consider now efficiency of mass transfer for given drop size distribution. One can use directly Eq.(43) as the reference one and calculate efficiency of mass transfer either based on experimental data or applying any model of mass transfer, specific for given process conditions.

$$eff_{k_L} = \frac{k_L}{k_{FL}(a_{drop}/a_{eq})} \quad (51)$$

where  $a_{eq}$  is the surface of a sphere with identical volume as the considered droplet.

As an example let us consider mass transfer of benzoic acid from toluene drops to aqueous solution in dense emulsion of volume fraction  $\phi = 0.75$  processed in a rotor-stator mixer as described by Baldyga et al. (2016).

2D numerical CFD simulations of the process in the in-line rotor-stator device for drops whose diameter falls within the inertial subrange of turbulence were carried out using the standard k- $\varepsilon$  model

of Fluent-Ansys and the multiple reference frame method (MRFR) linked to the population balance equation. Simulations were performed to predict the hydrodynamic properties of the flow, the size distribution of droplets forming emulsion, its viscosity and volumetric mass transfer coefficient. An unstructured mesh consisting of 178 845 cells and 180 309 nodes was applied. Gambit was used including application of its smoothing procedures to redistribute nodes, and the resulting drop sizes were mesh independent. Simulations were performed using a computer cluster consisting of 17 single-processor PCs and 7 double-processor nodes connected by a local network.

Figure 12 shows distribution of the time scale  $\tau_D$  as calculated from Eqs. (43) and (46). Based on Eq. (47) one can calculate the  $eff_a$  efficiency:  $eff_a \approx 0.15$  at  $N = 1000$  rpm and  $eff_a = 0.058$  at  $N = 11\ 000$  rpm.

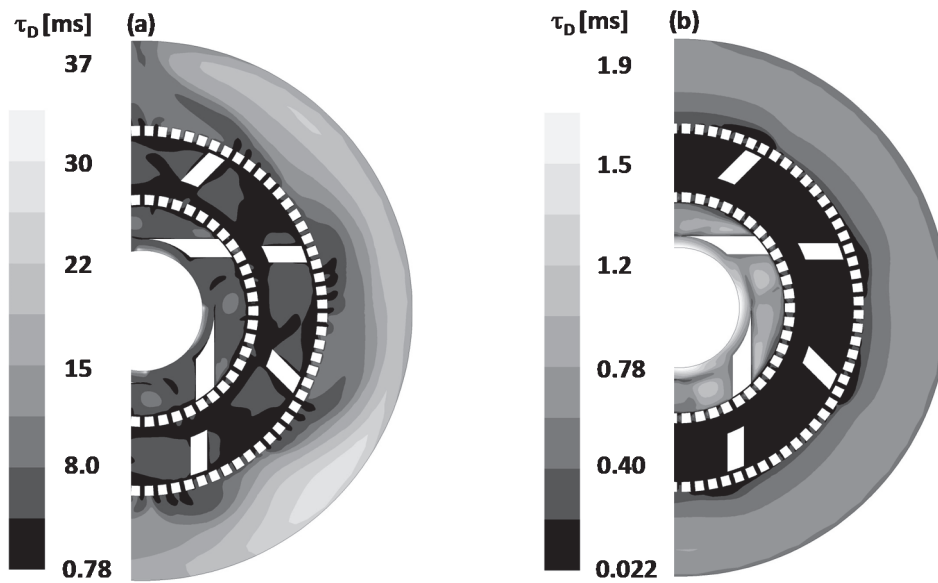


Fig. 12. The time constant for mass transfer of benzoic acid from toluene drops to aqueous solution emulsion for  $\varphi = 0.75$   $\eta_c = 0.91$  mPas,  $\eta_d = 0.587$  mPas,  $Q_m = 600$  kg/h (a)  $N = 1000$  rpm, (b)  $N = 11\ 000$  rpm

To illustrate how one can find  $eff_{k_L}$  let us consider effects of presence of surface-active contaminants in the system. Such impurities can eliminate internal circulation, thereby significantly reducing mass transfer rate. Assuming that droplets behave as hard spheres because of no internal circulation, one can use the model of Batchelor (1980) for  $k_L$ .

$$Sh = \frac{k_L R}{D_i} = 0.55 Pe^{1/3} = 0.55 \left( \frac{R^2 \varepsilon^{1/2}}{D_i \nu^{1/2}} \right)^{1/3} \quad (52)$$

with  $R = R_{32} = d_{32}/2$  and the Sauter mean diameter taken in the considered example from CFD results. Based on Eq.(48) we get for the mass transfer efficiency  $eff_{k_L} \approx 0.24$  at  $N = 1000$  rpm and  $eff_{k_L} = 0.19$  at  $N = 11\ 000$  rpm.

The general efficiency including both aspects of the process i.e. drop breakage and mass transfer, takes the values  $eff = eff_a \cdot eff_{k_L} = 0.036$  at  $N = 1000$  rpm and  $eff = eff_a \cdot eff_{k_L} = 0.011$  at  $N = 10\ 000$  rpm.

To check if turbulence is intensive enough to use the models developed for turbulent flow, the Reynolds number  $Re_L = \frac{u'L}{\nu}$  based on the scale of large, energy containing eddies is plotted in Fig. 13.

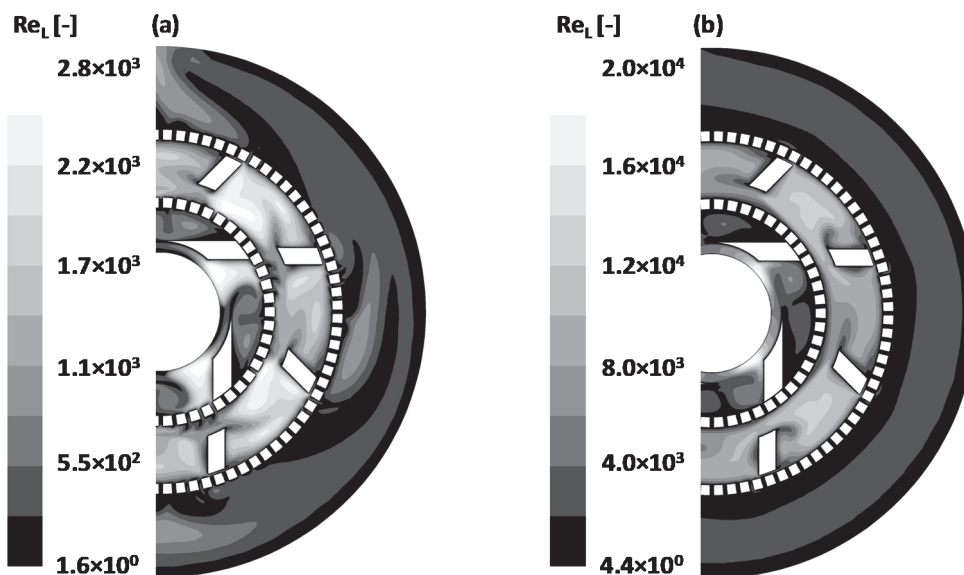


Fig. 13. The Reynolds number for emulsion flow for  $\varphi = 0.75$ ,  $\eta_c = 0.91$  mPas,  $\eta_d = 0.587$  mPas,  $Q_m = 600$  kg/h at  $N = 1000$  rpm, (b) at  $N = 11000$  rpm

Figure 13 shows that turbulence is well developed in most of the rotor-stator inside, especially in the rotor swept region, so the assumption on turbulent flow in the mixer is justified.

## 5. CONCLUSIONS

A new definition of efficiency of mixing in homogeneous systems is proposed, discussed and applied to interpret experimental data. The new definition represents modification and generalization to turbulent flows of a definition proposed originally by Ottino (1980). It has been shown that similar methods can be applied to investigate efficiency of drop breakage and mass transfer in two-phase liquid-liquid systems. Results show that the value of efficiency of mixing is not high in popular types of reactors and mixers, but can be used to compare different methods of contacting reactants and identify the mechanism of mixing.

*The authors acknowledge the financial support from Polish National Science Centre (Grant agreement number: DEC-2013/11/B/ST8/00258).*

## SYMBOLS

$a$	interfacial area per unit volume of emulsion, $\text{m}^{-1}$
$a_{drop}$	drop area, $\text{m}^2$
$a_v$	intermaterial area, $\text{m}^{-1}$
$c$	concentration, $\text{mol m}^{-3}$
$c_i$	concentration of component "i", $\text{mol m}^{-3}$
$D$	rotor diameter, m
$\bar{D}$	deformation tensor, $\text{s}^{-1}$
$D_i$	molecular diffusivity of component "i", $\text{m}^2 \text{s}^{-1}$
$d$	drop diameter, m
$d_d$	maximum stable drop size, m
$d_{32}$	Sauter diameter, m

$E$	engulfment parameter, $s^{-1}$
$eff$	efficiency
$I_{ij}$	concentration moments, $m^2$
$I_D$	concentration moment for pure diffusion, $m^2$
$I_{SD}$	concentration moment for diffusion and deformation, $m^2$
$K$	viscosity ratio, $K = \eta_d / \eta_c$
$K_L$	overall mass transfer coefficient, $m\ s$
$k_2$	rate constant of the 2 <sup>nd</sup> order chemical reaction, $m^3\ mol^{-1}\ s^{-1}$
$k_L$	mass transfer coefficient, $m\ s^{-1}$
$k_{Lc}$	mass transfer coefficient in continuous phase, $m\ s^{-1}$
$k_{Ld}$	mass transfer coefficient in dispersed phase, $m\ s^{-1}$
$L$	integral scale of turbulence, $m$
$N$	rotor speed, rps
$N_{Ca}$	capillary number, $\eta_c \dot{\gamma} d / \sigma$ ; for Eq.(43) $\eta_c \dot{\gamma} R_{eq} / \sigma$
$N_P$	power number, $P / (\rho N^3 D^5)$
$N_Q$	dimensionless pumping capacity, $Q / (ND^3)$
$P$	power, W
$P$	equilibrium distribution coefficient
$Pe$	Péclet number, $R^2 \dot{\gamma} D_i^{-1}$
$Re$	Reynolds number
$\underline{Q}$	volumetric flow rate, $m^3\ s^{-1}$
$\underline{Q}_m$	mass flow rate, $kg\ s^{-1}$
$R_{eq}$	equivalent radius, $m$
$Sc$	Schmidt number, $\nu D_i^{-1}$
$Sh$	Sherwood number, $k_L R D_i^{-1}$
$S$	skewness factor
$s_{ij}$	deformation tensor, $s^{-1}$
$t$	time, $s$
$\vec{u}$	velocity vector, $ms^{-1}$
$u_i$	component of velocity vector, $ms^{-1}$
$u'$	root-mean-square velocity component, $ms^{-1}$
$V_H$	rotor swept volume, $m^3$
$X_S, X_Q$	product distributions of complex reactions
$Y$	deformation parameter in Eq. (43), $Y = (19K + 16) / (16K + 16)$

### Greek symbols

$\alpha$	volume ratio
$\beta$	coefficient in definition of effective shear rate
$\varepsilon$	rate of energy dissipation, $m^2\ s^{-3}$
$\delta_0$	initial slab thickness, $m$
$\dot{\gamma}$	rate of shear, rate of elongation, $s^{-1}$
$\dot{\gamma}'$	rate of shear, $s^{-1}$
$\eta_d$	viscosity of dispersed phase, $Pa\ s$
$\eta_c$	viscosity of continuous phase, $Pa\ s$
$\Lambda_c$	integral scale for turbulent fluctuations of concentration, $m$
$\lambda$	striation thickness, $m$
$\lambda_B$	Batchelor microscale, $m$
$\lambda_K$	Kolmogorov microscale, $m$
$\nu$	kinematic viscosity, $m^2\ s^{-1}$

$\vec{\xi}$	position vector in a moving frame, m
$\rho_d$	density of dispersed phase, kg m <sup>-3</sup>
$\rho_c$	density of continuous phase, kg m <sup>-3</sup>
$\sigma$	[N m <sup>-1</sup> ] interfacial tension
$\tau_D$	time constant for mass transfer, N m <sup>-1</sup>
$\tau_M$	time constant for mixing, s
$\varphi$	volume fraction of dispersed phase
$\Omega_{ij}$	rotation tensor, s <sup>-1</sup>
$\vec{\omega}$	vorticity vector, s <sup>-1</sup>

## REFERENCES

- Baldyga J., Bourne J.R., 1986. Principles of micromixing, Chapter 6 In: Cheremisinoff N.P. (Ed.), *Encyclopedia of Fluid Mechanics*, Gulf Publishing Company, Houston, Texas, 1986.
- Baldyga, J., Jasińska M., Kowalski A.J., 2016. Effect of rheology of dense emulsions on the flow structure in agitated systems. *Chem. Eng. Res. Des.*, 108, 3-12. DOI:10.1016/j.cherd.2015.11.026.
- Baldyga J., Podgórska W., 1998. Drop break-up in intermittent turbulence: Maximum stable and transient sizes of drops. *The Canadian J. Chem. Eng.*, 76, 456-470. DOI: 10.1002/cjce.5450760316.
- Baldyga J., Bourne J.R., 1999. *Turbulent Mixing and Chemical Reactions*. Wiley, Chichester.
- Batchelor G.K., 1980. Mass transfer from small particles suspended in turbulent flow. *J. Fluid. Mech.*, 98, 609-623. DOI: 10.1017/S0022112080000304.
- Bourne J.R., Kut O.M., Lenzner J., 1992. An Improved reaction system to investigate micromixing in high-intensity mixers. *Ind. Eng. Chem. Res.*, 31, 949-958. DOI: 10.1021/ie00003a042.
- Bourne J.R., 2003. Mixing and the selectivity of chemical reactions. *Org. Proc. Res. Dev.*, 7, 471-508. DOI: 10.1021/op020074q.
- Corrsin S., 1964. Further generalizations of Onsager's cascade model for turbulent spectra. *Phys. Fluids*, 7, 1156-1159. DOI: 10.1063/1.1711355.
- Falk L., Commenge J.-M., 2010. Performance comparison of micromixers. *Chem. Eng. Sci.*, 65, 405-411. DOI: 10.1016/j.ces.2009.05.045.
- Favelukis M., Lavrenteva O. M., 2013. Mass transfer around prolate spheroidal drops in an extensional flow. *Can. J. Chem. Eng.*, 91, 1190-1199. DOI: 10.1002/cjce.21727.
- Jasińska M., Baldyga J., Cooke M., Kowalski A.J., 2013a. Application of test reactions to study micromixing in the rotor-stator mixer (test reactions for rotor-stator mixer). *Appl. Therm. Eng.*, 57, 172-179. DOI: 10.1016/j.applthermaleng.2012.06.036.
- Jasińska M., Baldyga J., Cooke M., Kowalski A.J., 2013b. Investigations of mass transfer with chemical reactions in two-phase liquid-liquid systems. *Chem. Eng. Res. Des.*, 91, 2169-2178. DOI: 10.1016/j.cherd.2013.05.010.
- Levenspiel O., *Chemical Reaction Engineering*. Wiley, New York 1972.
- Malecha K., Golonka L.J., Baldyga J., Jasińska M., Sobieszuk P., 2009. Serpentine microfluidic mixer made in LTCC. *Sens. Actuators B: Chem.*, 143, 400-413. DOI: 10.1016/j.snb.2009.08.010.
- Ottino J.M., 1980. An efficiency for batch mixing of viscous fluids. *Chem. Eng. Sci.*, 35, 1454-1457. DOI: 10.1016/0009-2509(80)85142-6.
- Rozeń A., 2008. *Micromixing of fluids differing in viscosity in laminar flow systems*. Oficyna Wydawnicza Politechniki Warszawskiej, Warsaw.
- Tennekes H., Lumley J.L., 1972. *A first course in turbulence*. MIT Press, Cambridge, MA, USA.
- Villermaux, J., 1986. Micromixing phenomena in stirred reactors. Chapter 27 In: *Encyclopedia of Fluid Mech.* Gulf Publishing Company, Houston, TX.

*Received 3 December 2016*

*Received in revised form 27 August 2017*

*Accepted 28 August 2017*